



Published in final edited form as:

Oncogene. 2017 August 31; 36(35): 4997–5005. doi:10.1038/onc.2017.117.

INTU is essential for oncogenic Hh signaling through regulating primary cilia formation in basal cell carcinoma (BCC)

Ning Yang¹, Elaine Lai-Han Leung², Chengbao Liu¹, Li Li³, Thibaut Eguether⁴, Xiao Jun Yao², Evan C. Jones⁵, David A. Norris⁶, Aimin Liu⁷, Richard A. Clark⁵, Dennis R. Roop^{6,8}, Gregory J. Pazour⁴, Kenneth R. Shroyer¹, and Jiang Chen^{1,5,*}

¹Department of Pathology, Stony Brook University, Stony Brook, NY

²State Key Laboratory of Quality Research in Chinese Medicine, Macau University of Science and Technology, Macau, China

³Department of Dermatology, Peking Union Medical College Hospital, Beijing, China

⁴Program in Molecular Medicine, University of Massachusetts Medical School, Worcester, MA 01605

⁵Department of Dermatology, Stony Brook University, Stony Brook, NY

⁶Charles C. Gates Center for Regenerative Medicine, University of Colorado Denver, Aurora, CO

⁷Department of Biology, Eberly College of Science, Pennsylvania State University, University Park, PA

⁸Department of Dermatology, University of Colorado Denver, Aurora, CO

Abstract

Inturned (INTU), a cilia and planar polarity effector (CPLANE), performs prominent ciliogenic functions during morphogenesis, such as in the skin. INTU is expressed in adult tissues but its role in tissue maintenance is unknown. Here, we report that the expression of the *INTU* gene is aberrantly elevated in human basal cell carcinoma (BCC), coinciding with increased primary cilia formation and activated hedgehog (Hh) signaling. Disrupting *Intu* in an oncogenic mutant Smo (*SmoM2*)-driven BCC mouse model prevented the formation of BCC through suppressing primary cilia formation and Hh signaling, suggesting that *Intu* performs a permissive role during BCC formation. INTU is essential for IFT-A complex assembly during ciliogenesis. To further determine whether *Intu* is directly involved in the activation of Hh signaling downstream of ciliogenesis, we examined the Hh signaling pathway in mouse embryonic fibroblasts, which readily respond to Hh pathway activation. Depleting *Intu* blocked SAG-induced Hh pathway activation, whereas the expression of Gli2^N, a constitutively active Gli2, restored Hh pathway activation in *Intu*-deficient cells, suggesting that INTU functions upstream of Gli2 activation. In

Users may view, print, copy, and download text and data-mine the content in such documents, for the purposes of academic research, subject always to the full Conditions of use: http://www.nature.com/authors/editorial_policies/license.html#terms

*Correspondence: Jiang Chen, MD, Department of Pathology, Stony Brook University School of Medicine, Basic Science Tower, Level 9, Room 151, Stony Brook, NY 11794, Phone: 631-444-3199, Fax: 631-444-6487, jiang.chen@stonybrook.edu.

CONFLICT OF INTEREST

The authors state no conflict of interest.

contrast, overexpressing *Intu* did not promote ciliogenesis or Hh signaling. Taken together, data obtained from this study suggest that INTU is indispensable during BCC tumorigenesis and that its aberrant upregulation is likely a prerequisite for primary cilia formation during Hh-dependent tumorigenesis.

Keywords

INTU; BCC; cilia; hedgehog; skin; keratinocyte

INTRODUCTION

Inturned (INTU) is a tissue-specific planar cell polarity (PCP) effector. It mediates the polarity cues set up by the core PCP components in *Drosophila* and vertebrate animals¹. During vertebrate morphogenesis, INTU also exerts prominent functions in primary cilia formation. Disrupting the *Intu* gene in mice can cause defects in neural tube formation, limb patterning, and hair follicle morphogenesis, all of which are associated with impaired cilia formation or function²⁻⁶. Mechanistically, INTU forms a molecular module with the other two PCP effectors, Fuzzy (FUZ) and WDPCP, to facilitate the assembly of intraflagellar transport A (IFT-A) peripheral proteins into the IFT-A complex to facilitate cilia formation during vertebrate morphogenesis⁷. Because of their prominent functions in PCP and ciliogenesis, these PCP effectors are recognized as cilia and planar polarity effectors (CPLANEs). However, their roles in tissue homeostasis are unclear.

Basal cell carcinoma (BCC) of the skin is the most common malignancy in the United States, with more than 2.8 million new diagnoses annually. BCC originates from epidermal keratinocytes and is caused predominantly by loss-of-function mutations in the patched 1 (*PTCH1*)^{8,9} or gain-of-function mutations in the smoothened (*SMO*) gene¹⁰, which encodes upstream transmembrane components of the hedgehog (Hh) signaling pathway. Oncogenic mutations in *PTCH1* or *SMO* ultimately lead to uncontrolled activation of the glioma-associated oncogene (Gli) transcription factors, thus, the Hh signaling pathway¹¹.

The activation of the Hh signaling pathway is dependent on the primary cilium, a cellular organelle that is essential for the translocation of Hh pathway components and the subsequent activation of the Hh target genes, such as *Gli1* and *Ptch1*^{12,13}. The functional importance of primary cilia for the Hh signaling pathway is well-established during both morphogenesis¹³⁻¹⁵ and the formation of Hh-dependent tumors, such as medulloblastoma¹⁶ and BCC¹⁷.

To gain insight into the function of the CPLANEs during mammalian tissue homeostasis, we explored the functions of INTU in the context of BCC formation. We found that the *INTU* gene is aberrantly upregulated in human BCC specimens and that genetically ablating the endogenous *Intu* in a BCC mouse model blocked BCC formation, likely upstream of the activation of Gli transcription factors. These observations suggest that INTU, which is essential for ciliogenesis, plays a permissive role during the development of BCC.

RESULTS

INTU is upregulated in human BCC

To determine whether INTU is involved in epidermal homeostasis, we constructed a tissue microarray (TMA) comprised of healthy human skin, BCC, and squamous cell carcinoma (SCC) specimens (Supplementary Fig. 1a), and examined the transcriptional levels of the endogenous *INTU* gene by *in situ* hybridization. In healthy adult epidermis, *INTU* is predominantly expressed in interfollicular and follicular epidermal keratinocytes at a relatively modest level in comparison to embryonic skin (Figure 1a and b and Supplementary Figure 1b). Strikingly, *INTU* expression was markedly elevated in BCC tumors (n = 19, $P < 0.05$), but not in SCCs (n = 3), when compared to healthy adult skins (n = 3) (Figure 1a and b). As expected, the transcription level of *PTCHI*, an Hh responsive genes, was also significantly elevated in BCC ($P < 0.001$), but not SCC, a type of keratinocyte carcinoma that is not dependent on Hh signaling (Figure 1a and c). *GLII*, another Hh-responsive gene, exhibited a similar trend (Figure 1a and d). In contrast, the level of *SMO*, which is not an Hh responsive gene, was unchanged (Figure 1a and e). Moreover, the relative expression levels of *INTU* correlated with that of *PTCHI* (Spearman $r = 0.784$, $P < 0.001$) or *GLII* (Spearman $r = 0.858$, $P < 0.001$), but not with *SMO* (Supplementary Figure 2a – c), suggesting that elevated level of *INTU* is associated with activation of the Hh signaling pathway in human skin.

Human BCCs comprise abundant ciliated keratinocytes

It was reported that the primary cilia were frequently observed in BCC¹⁷. To determine the prevalence of ciliated cells in human BCC, we evaluated the abundance of primary cilia in the same cohort of human skin specimens described above by immunofluorescence labeling. A significantly increased proportion ($38.5 \pm 13.3\%$) of BCC cells possesses a primary cilium in comparison to keratinocytes ($2.5 \pm 2.2\%$) in healthy skins or SCCs ($2.4 \pm 0.6\%$) (Figure 1f and g, $P < 0.001$), suggesting that the primary cilium may be a biomarker for BCC. Moreover, the abundance of ciliated cells also appeared correlated with the relative expression levels of *INTU* (Spearman $r = 0.668$, $P < 0.001$, Supplementary Figure 2d). This observation suggested that the ciliogenic program is likely upregulated in BCC cells, which may be related to the elevated levels of *INTU* and the activated Hh signaling pathway.

Intu is essential for BCC formation

INTU is essential for primary cilia formation and the activation of the Hh signaling pathway during skin morphogenesis⁶. Elevated *INTU* expression, along with increased primary cilia formation and the aberrant activation of the Hh pathway, in BCC suggests that INTU may be functionally required for BCC formation. To test this idea, we engineered a BCC mouse model (*Krt14-Cre^{ERT};SmoM2^{cond};Intu^{flox/flox}*), which permits the simultaneous expression of an oncogenic mutant SmoM2 (*SmoM2^{cond}*) and the ablation of the endogenous *Intu* locus (*Intu^{flox/flox}*) through tamoxifen-induced activation of Cre recombinase in keratinocytes.

Initial tamoxifen treatment was carried out on 3-week old littermates. By five weeks, control mice that were heterozygous for the conditional allele of *Intu* (*Krt14-Cre^{ERT};SmoM2^{cond};Intu^{+/flox}*) started to exhibit signs of various skin abnormalities,

including hair loss, scaly skin, bumpy tails, and crumpled ears (data not shown). By 10 weeks, these skin phenotypes exacerbated and progressed to extensive skin erosion (Figure 2a and b), thus, the control mice had to be euthanized. Histologically, dorsal skins of control mice revealed remarkable downward growth of hyperplastic keratinocytes (Figure 2b). Consistent with previous reports¹⁷⁻¹⁹, these cells exhibited features of human BCC, such as basaloid appearance, high nuclear to cytoplasmic ratio, and palisading nuclei (Supplementary Figure 3a). Immunofluorescence labeling confirmed that these cells coexpressed KRT14 and KRT17 (Supplementary Figure 3b), which is characteristic of BCC. Moreover, these BCC-like cells were positive for yellow fluorescence protein (YFP, Figure 2c, upper and middle panels), which was coexpressed with SmoM2 as a fusion protein, thereby confirming that they were indeed derived from cells expressing SmoM2. Overall, these BCC-like lesions were reminiscent of human BCC. *In situ* hybridization confirmed that the endogenous *Intu* is abundantly expressed in these lesions (Figure 2c).

In contrast, littermates homozygous for the conditional allele of *Intu* (*Krt14-Cre^{ERT};SmoM2^{cond};Intu^{flox/flox}*) did not show gross signs of BCC formation even by 22 weeks (or 154 days) after tamoxifen induction (Figure 2a and b upper panels). Thus, disease-free survival of these mutant mice homozygous for *Intu* was significantly different than that of the control littermates (Logrank test $P < 0.0001$, Figure 2a). Histologically, the dorsal skins of homozygous mice exhibited rather mild hyperplasia and focal dysplasia (Figure 2b, lower panels, arrow). YFP and KRT14 staining confirmed that keratinocytes of these mice expressed oncogenic *SmoM2* (Figure 2c), whereas *in situ* hybridization demonstrated markedly diminished expression of *Intu* (Figure 2c, lower panels), suggesting that *Intu* is required for the formation of oncogenic SmoM2-driven BCC.

Histologically, *Krt14-Cre^{ERT};SmoM2^{cond};Intu^{flox/flox}* mice exhibited consistently thinner interfollicular epidermis (IFE) in comparison to controls (*Krt14-Cre^{ERT};SmoM2^{cond};Intu^{+/-flox}*) (Figure 2d, $P < 0.001$). The thickness of IFE of BCC mouse models homozygous for *Intu* conditional allele remained constant up to 22 weeks after tamoxifen induction (Figure 2d), suggesting genetically ablating *Intu* blocked, rather than delayed, BCC formation.

Moreover, the epidermis of *Krt14-Cre^{ERT};SmoM2^{cond};Intu^{flox/flox}* mice maintained normal KRT17 expressing pattern (Supplementary Figure 3b). BrdU labeling demonstrated that *Krt14-Cre^{ERT};SmoM2^{cond};Intu^{+/-flox}* skins harbored substantially more proliferating keratinocytes (KRT14-positive) than those of *Krt14-Cre^{ERT};SmoM2^{cond};Intu^{flox/flox}* mice ($7.06 \pm 0.49\%$ vs $1.61 \pm 0.41\%$, Figure 2e and Supplementary Figure 3c). Taken together, these data demonstrated that genetically ablating *Intu* in the epidermis can protect mice from developing BCC-like lesions induced by the oncogenic SmoM2, suggesting that *Intu* plays a permissive role during BCC formation.

***Intu* is required for primary cilia formation in BCC**

Primary cilia are abundant in human BCC (Figure 1f and g) and are essential for Hh signaling. Therefore, it was speculated that cells in the BCC-like lesions in control mice are likely to be ciliated. Indeed, BCC-like lesions in *Krt14-Cre^{ERT};SmoM2^{cond};Intu^{+/-flox}* mice contained abundant ciliated keratinocytes ($34.9 \pm 6.7\%$, Figure 3a), at a proportion similar to

what was observed in human BCC ($38.5 \pm 13.3\%$, Figure 1g). These findings not only suggest that the *SmoM2* mouse models are able to recapitulate cellular features of human BCC, but also suggest that upregulated cilia formation is an intrinsic feature of BCC.

Given the essential role of INTU in ciliogenesis, particularly in epidermal keratinocytes ⁶, we postulated that disrupting *Intu* might block BCC formation through impairing ciliogenesis. Indeed, homozygous *Intu* mutants (*Krt14-Cre^{ERT};SmoM2^{cond};Intu^{flox/flox}*) contained few ciliated epidermal keratinocytes ($8.8 \pm 1.4\%$), reminiscent of those not expressing *SmoM2* ($9.4 \pm 1.1\%$, *Krt14-Cre^{ERT};Intu^{+ /flox}*, Figure 3a). These observations suggested that *Intu* might be required for BCC formation through facilitating ciliogenesis.

Intu* is required for the activation of Hh signaling in BCC *in vivo

Unrestricted activation of Hh signaling is the primary molecular driver for BCC. To determine whether *Intu* is required for the activation of the Hh signaling pathway during BCC formation, we examined Hh target genes (*Gli1* and *Ptch1*) in the *SmoM2*-driven BCC mouse models. *In situ* hybridization demonstrated that *Gli1* and *Ptch1* transcripts were markedly elevated in BCC-like lesions of control mice (*Krt14-Cre^{ERT};SmoM2^{cond};Intu^{+ /flox}*), but attenuated in homozygous *Krt14-Cre^{ERT};SmoM2^{cond};Intu^{flox/flox}* mice (Figure 3b). In response to Hh pathway activation, canonical Wnt signaling is also activated in BCC. Indeed, nuclear LEF1, a marker for activated Wnt signaling, was expressed in cells of the BCC-like lesions of control (*Krt14-Cre^{ERT};SmoM2^{cond};Intu^{+ /flox}*) mice, but nearly undetectable in the skin of homozygous (*Krt14-Cre^{ERT};SmoM2^{cond};Intu^{flox/flox}*) mice, except in dermal papilla (DP) cells (Figure 3c). These data suggest that *Intu* is required for the activation of the Hh signaling pathway during the development of *SmoM2*-driven BCC *in vivo*.

Intu* is required for SmoM2-mediated Hh pathway activation in keratinocytes *in vitro

To further determine whether *Intu* is required for Hh pathway activation ensuing the expression of oncogenic *Smo* gene, we examined the expression of Hh target genes in primary keratinocytes harboring the inducible *SmoM2* allele. Five days after 4-OH tamoxifen induction, *Gli1* transcription was robustly upregulated in keratinocytes isolated from *Krt14-Cre^{ERT};SmoM2^{cond};Intu^{+ /flox}* mice in comparison to those isolated from control mice (*SmoM2^{cond};Intu^{+ /flox}*) (Figure 4a). Whereas such induction was essentially abolished in cells isolated from mice homozygous for the conditional *Intu* allele (*Krt14-Cre^{ERT};SmoM2^{cond};Intu^{flox/flox}*) ($P < 0.05$, Figure 4a). Quantification of the transcriptional levels of *Intu* confirmed that the attenuated induction of *Gli1* was indeed associated with diminished levels of *Intu* (Figure 4a). These findings suggest that *Intu* is required for keratinocyte to activate the Hh signaling pathway in response to the expression of oncogenic *SmoM2*.

To determine whether the Hh phenotype of *Intu*-deficient keratinocytes is corroborated with impaired ciliogenesis, we examined the primary cilia by immunofluorescence. In 4-OH tamoxifen activated control cells (*Krt14-Cre^{ERT};SmoM2^{cond};Intu^{+ /flox}*, left, indicated by *), *SmoM2* was activated as demonstrated by YFP. Primary cilium was readily detectable in $49.9 \pm 2.8\%$ control cells (Figure 4b – c). Moreover, *SmoM2* appeared enriched at the

primary cilium such that triple fluorescence labeling makes the cilium appear white (Figure 4b, indicated by an arrow head). In contrast, in keratinocytes homozygous for the conditional allele of *Intu* (*Krt14-Cre^{ERT};SmoM2^{cond};Intu^{flox/flox}*), 4-OH tamoxifen activated the expression of SmoM2, as demonstrated by YFP expression (Figure 4b, right, indicated by *), but the formation of primary cilium was only observed in $25.8 \pm 1.7\%$ cells ($P < 0.05$, Figure 4c). Interestingly, primary cilia formation (Figure 4b, right, indicated by an arrow) appeared unaffected in *Krt14-Cre^{ERT};SmoM2^{cond};Intu^{+/-flox}* or *Krt14-Cre^{ERT};SmoM2^{cond};Intu^{flox/flox}* cells that did not undergo Cre-mediated recombination, as judged by the lack of YFP expression ($42.3 \pm 8.9\%$ and $47.1 \pm 8.8\%$, respectively) (Figure 4c). The ciliated *Krt14-Cre^{ERT};SmoM2^{cond};Intu^{flox/flox}* cells (Figure 4b, right, indicated by p) presumably retained the endogenous *Intu* due to insufficient Cre-mediated recombination. These results suggested that *Intu* is essential for primary cilia formation irrespective of the expression of oncogenic *SmoM2*.

In summary, these *in vitro* experiments suggested that *Intu* is a key component of both ciliogenesis and the *SmoM2*-activated oncogenic Hh signaling.

***Intu* acts upstream of the Gli transcription factors**

Data obtained so far in BCC was in line with prior findings that *Intu* is required for Hh pathway activation at the level of primary cilia. To examine whether *Intu* is also involved in the activation of the Hh signaling downstream of primary cilia, we examined Hh pathway in mouse embryonic fibroblasts (MEFs) that readily form primary cilia after serum starvation and respond to Hh pathway activation. First, we found that *Intu^{-/-}* MEFs exhibited strong primary cilia phenotypes such that ciliogenesis was almost completely suppressed ($0.52 \pm 0.53\%$) when compared with wild type MEFs ($61.2 \pm 1.9\%$) ($P < 0.001$, Fig. 5a). Moreover, the Smo Agonist (SAG)-mediated Hh pathway activation was severely attenuated in *Intu^{-/-}* MEFs in comparison to control wild type MEFs, as determined by the processing of full-length GLI3 (GLI3-FL) to GLI3 repressor (GLI3-R) (Figure 5b), as well as the transcription levels of *Gli1* and *Ptch1* (Figure 5c – d, columns indicated by V). These results suggest that *Intu* is required for Smo-mediated Hh pathway activation.

To determine whether *Intu* is also involved in the molecular signaling machinery downstream of Smo, we used plasmids expressing inactive full-length Gli2 (Gli2-FL) and a constitutively active Gli2 (Gli2^N 1-413 or Gli2^N) to rescue the Hh pathway in *Intu^{-/-}* MEFs. First, Gli2^N, but not Gli2-FL, consistently elicited Hh pathway activation in wild type and *Intu^{-/-}* MEFs, as determined by *Gli1* and *Ptch1* transcription (Supplementary Figure 4, and Figure 5c – d, open bars), suggesting that INTU functions upstream of GLI2 and is dispensable for Gli2^N-induced Hh pathway activation. When this experiment was conducted in conjunction with SAG, Gli2^N was unable to further activate Hh signaling in *Intu^{-/-}* MEFs, as determined by *Gli1* and *Ptch1* transcription (Figure 5c – d, solid bars). This result conforms to the prior findings that *Intu* is required for SMO activation. The overexpression of Gli2-FL and Gli2^N was robust as confirmed in Figure 5e. Collectively, these findings suggested that INTU acts upstream of Gli2 to facilitate oncogenic SMO-mediated Hh pathway activation.

To further determine whether elevated INTU levels might be sufficient to drive ciliogenesis and Hh pathway activation, we overexpressed mouse *Intu* that was fused with GFP (*mIntu*)⁵ in wild type MEFs. *Intu* was robustly overexpressed in MEFs (Figure 5f – g), but ciliogenesis was not increased (Figure 5f). Similarly, the level of endogenous Hh target genes, such as *Ptch1*, was also not increased (Figure 5h). These data do not support INTU as a driver for ciliogenesis or Hh pathway activation. Thus, the elevated expression of *INTU* in human BCCs might be required but not sufficient for the development of tumors.

DISCUSSION

The ciliogenic functions of the CPLANE genes (*Fuz*, *Wdpcp*, and *Intu*) are indispensable during vertebrate morphogenesis^{4–6, 20–25}. The current study extended their biological functions to mammalian tumorigenesis by demonstrating that INTU plays a permissive role in BCC formation through regulating primary cilia formation and Hh signaling. Because that the CPLANEs form a molecular module by interacting physically to facilitate the assembly of the IFT-A complex during ciliogenesis⁷, it is speculated that genetically disrupting other CPLANE genes may block BCC formation in a fashion similar to *Intu*.

The robust upregulation of *INTU* transcription in BCC cells was surprising. It is not only in concert with the idea that INTU is prerequisite for ciliogenesis, but also suggests that INTU is required for the propagation and maintenance of ciliated BCC cells. While we did not obtain evidence supporting a role of INTU in directly driving ciliogenesis or Hh signaling (Figure 5g–h), it is of interest to know that the expression level of *INTU* correlates with those of Hh responsive genes and ciliogenesis in BCC specimens (Supplementary Figure 3). These observations suggest that INTU acts in concert with other molecular events to promote ciliogenesis and Hh pathway activation in BCC.

It remains unknown how *INTU* is upregulated in BCC. It may be a mere reflection of the increased proportion of ciliated BCC cells that already express relatively high endogenous levels of *INTU*. It is also possible that the expression of oncogenic mutant Hh genes, such as *PTCH1*, *SMO* or *Gli2*, may drive *de novo* upregulation of *INTU*, and probably other ciliogenic genes, to deregulate the ciliogenic and retraction programs to favor cilia formation in keratinocytes. Another possible mechanism is UV, a primary risk factor for BCC²⁶ and a robust inducer of ciliogenesis²⁷. UV may exert previously unappreciated ciliogenic functions during the early stages of BCC formation. Understanding how *INTU* is upregulated may provide important insight into BCC tumorigenesis.

Previous observations suggested that very few interfollicular epidermal keratinocytes in adult skin possess a functional cilium, whereas BCC cells are frequently ciliated^{6, 17, 28}. Indeed, quantifications obtained in this study confirmed these findings, thereby suggest that primary cilium is a candidate biomarker for BCC. But it is unclear how BCC cells acquired the cilia phenotype. In addition to the altered intrinsic ciliogenic programs discussed above, it is also possible that BCC originates from the few ciliated keratinocytes. It is conceivable that ciliated keratinocytes can activate the Hh signaling pathway more readily upon acquiring Hh pathway mutations, thereby, may gain growth advantage over unciliated keratinocytes. Thus, these findings provided insight into the debated origin of

BCC^{18, 19, 29–32} by suggesting that BCC may be more readily established from ciliated keratinocytes in the skin and hair follicles. Collectively, evidence supports the idea that ciliated keratinocytes are prone, whereas unciliated keratinocytes are resistant, to malignant transformation of keratinocytes.

Activation of the Hh pathway, which is a major driver of BCC, is dependent upon the primary cilium. The primary cilium is critical for BCC formation as we and others demonstrated that preventing cilia assembly by genetically ablating ciliogenic genes, such as *Ift88*, *Kif3a*, and *Intu* prevented BCC⁽¹⁷ and this study) could block the development of BCC in mice. These findings suggest that ciliogenic proteins might be therapeutic targets for BCC. However, systemically targeting INTU and other ciliogenic proteins is likely to result in significant adverse effects on the normal ciliary functions, such as those in the retina, kidney, and other organs. Therefore, this strategy is unlikely worthwhile. In contrast, targeting SMO with small molecules is remarkably effective for locally advanced or metastatic BCCs³³. However, the development of treatment-resistant tumors in association with SMO inhibitor treatment^{34–37} presses for the identification of new therapeutic targets along the Hh signaling pathway^{38, 39}. Thus, targeting Hh signaling components downstream of ciliogenesis and the smoothed receptor may become promising therapeutic strategies for BCC and other Hh-dependent cancers^{40–42}.

In summary, this study provided evidence that ciliogenic genes, such as *INTU*, are dynamically regulated in the skin, and that the upregulation of *INTU* is required but not sufficient for ciliogenesis and oncogenic Hh signaling during BCC formation. Understanding the molecular mechanism underlying with the aberrant upregulation of ciliogenic genes, such as *INTU*, during early stages of BCC formation may shed light on the prevention of BCC and other Hh-dependent tumors.

MATERIALS AND METHODS

Skin and BCC specimens

Formalin-fixed and paraffin-embedded healthy adult human skin, BCC, and SCC specimens (n = 25) were obtained from the biobank of the Department of Pathology. All specimens were de-identified. The use of human specimens was approved by the Institutional Review Board of Stony Brook University. Tumor histology was confirmed and areas of interest were chosen by two pathologists (CL and KRS) before they were used for the construction of a tissue microarray (TMA). Two cores of each specimen were randomly placed in the TMA block. All the staining and analyses were performed using slides sectioned from the TMA. One BCC specimen was lost during this process and was excluded. The TMA was comprised of 3 healthy skins, 19 BCCs, and 3 SCCs.

Mouse models and tissue collection

The conditional mouse model of *Intu* (*Intu^{flx/flx}*) were reported previously⁵. Tg(KRT14-cre/ERT)20Efu/J and Gt(ROSA)26Sor^{tm1(Smo/EYFP)Amc/J} (a conditional allele of *Smo*, also known as *SmoM2^{Cond}*) mice were obtained from the Jackson Laboratory (Bar Harbor, ME, USA). Mice were bred to generate the bigenic or trigenic mice used in the study. Littermates

were used as controls wherever possible. Both male and female mice were included in this study, and housed in groups of the same age and sex regardless of genotypes. Cre recombination was induced by tamoxifen (T5648, Sigma-Aldrich, St. Louis, MO) as described previously¹⁸. Briefly, 2.5 mg tamoxifen (dissolved in sesame oil) was injected intraperitoneally to 22 – 27 day old mice once daily for five days. BrdU labeling was performed by injecting 10 µg per gram of body weight of BrdU labeling reagent (Life Technologies, Waltham, MA) 2 hours prior to euthanasia. Injections were carried out blindly.

Based on our experience gained from a pilot study, we collected skin specimens from mice at two time points after tamoxifen induction. Additional time points were applied on *Intu*-deficient (*Krt14-Cre^{ERT};SmoM2^{cond};Intu^{flox/flox}*) mice up to 22 weeks after induction. We aimed to obtain a minimum of three mice for each time point. Freshly dissected dorsal skins were either frozen in optimal cutting temperature compound (Sakura Finetek USA, Torrance, CA) or fixed overnight in 10% buffered formalin and processed for routine histology. All procedures related to mice were approved by the IACUC of Stony Brook University.

Measuring the thickness of the epidermis

Three randomly chosen fields of each H&E section were photographed with a 20X objectives, and the thickness of the interfollicular epidermis (IFE) was measured using Nikon (Melville, NY) NIS-Elements Analysis D software. The average epidermal thickness from each mouse was used for analysis. Specifically, n = 9 or 18 for *Krt14-Cre^{ERT};SmoM2^{cond};Intu^{+/flox}* mice at 5 weeks or 10 weeks post induction, respectively; n = 9, 12, or 18 for *Krt14-Cre^{ERT};SmoM2^{cond};Intu^{flox/flox}* mice at 5, 10, or 22 weeks post induction.

Cell culture and *in vitro* assays

The isolation of primary mouse epidermal keratinocyte was conducted as described elsewhere⁴³. Briefly, skins of E18.5 embryos were digested by dispase II (Roche, Indianapolis, IN) to separate epidermis and dermis. Epidermis was then digested briefly with trypsin (Invitrogen) to dissociate keratinocytes. Keratinocytes were suspended in defined keratinocyte serum-free medium (Gibco, Life Technologies Waltham, MA) and plated on collagen I-coated tissue culture plates (Thermo Fisher, Waltham, MA). MEFs were cultured with Dulbecco's modified Eagle's medium (4.5 g/l glucose) supplemented with 10% fetal bovine serum and 100 U/ml penicillin and 100 U/ml streptomycin (Gibco, Life Technologies). To induce Cre recombination, subconfluent keratinocytes were treated with 0.5 µM 4-OH tamoxifen (Sigma-Aldrich) for 5 hours before grown to near-confluent, and starved in medium without growth supplement for 72 hours before harvested for RNA extraction or immunofluorescence. To activate Hh signaling, MEFs were grown to confluency and serum-starved in medium containing 0.25% serum for 24 hours, then treated with 400 nM smoothened agonist (SAG, Calbiochem, San Diego, CA) for 4.5 hours before harvested for mRNA extraction.

DNA constructs and transfection

Expression plasmid encoding *Intu*, full length mouse *Gli2* (Gli2-FL), and the constitutively active *Gli2* lacking the coding sequence for the first 413 amino acids (Gli2 N) were described previously^{5, 44}. GLI2 was expressed as a fusion protein with YFP. The transfections were carried out by Lipofectamine 2000 (Thermo Fisher Scientific, Waltham, MA) per manufacturer's instructions.

Quantitative RT-PCR

RNA isolation and quantitative RT-PCR analyses were performed as previously described⁶. The following TaqMan probes were used: *Ptch1*, Mm00436026_m1; *Gli1*, Mm00494645_m1; *Gli2*, Mm01293111_m1; *Intu*, Mm01284303_m1; and *β-actin*, Mm00607939_m1 (Life Technologies). Results were analyzed using the Ct method. Relative expression levels of target genes were normalized with *β-actin* and compared with controls.

In situ hybridization and scoring

In situ hybridization was carried out on formalin-fixed paraffin embedded tissue sections using the RNAScope system (Advanced Cell Diagnostic, Inc, Hayward, CA) per manufacturer's instructions. The probes used are *INTU* (413571), *GLI1* (310991), *PTCH1* (405781), *SMO* (405831), *Intu* (413601), *Gli1* (311001), and *Ptch1* (402811).

Semi-quantitative scoring was performed for signaling generated by each target probe on all TMA specimens. Scoring was based on the average number of signal puncta within a cell's boundary. *POLR2A* (Cat 310451) was used as an internal positive control for the quality of each specimen for this assay. Scores of each target probe were then normalized by *POLR2A*. Normalized scores of the randomly placed cores of the same specimen were averaged and presented. Scoring was performed by the investigators blind to the protocol.

Immunofluorescence labeling and microscopy

Immunofluorescence labeling was performed as described previously⁶. The following primary antibodies were used: antibody to KRT1 was produced in the Roop lab⁴⁵; KRT14 (Covance; Princeton, NJ); GFP/YFP (Aves Labs Inc; Tigard, Oregon); KRT17 (Abcam, Cambridge, MA, USA); LEF1 (Cell Signaling, Danvers, MA); BrdU (Life Technologies); acetylated α -tubulin (Sigma); γ -tubulin (Abcam, Cambridge, MA), ARL13B (NeuroMab, 73-287; Davis, CA); AlexaFluor-conjugated secondary antibodies were from Life Technologies. Mounting medium with DAPI (Vector Laboratories, Burlingame, CA) was used. Images were acquired by Nikon 80i fitted with Nikon DS-Qi1Mc camera and processed with Photoshop 5.5 CS.

Statistical analyses

All quantifications are presented as mean \pm SD. Student t-test (two-tail, unpaired, assuming unequal variance) was used unless otherwise stated. Kaplan-Meier curve, one-way ANOVA, two-way ANOVA analyses were generated by the GraphPad software (GraphPad Software, Inc., San Diego, CA). $P < 0.05$ is considered statistically significant.

Supplementary Material

Refer to Web version on PubMed Central for supplementary material.

Acknowledgments

We thank Stephanie Burke and Mallory Korman for histology assistance. This study is supported by the Research Histology Core Laboratory of the Department of Pathology, the Cancer Center of Stony Brook University, and a research grant from NIH (AR061485 to JC; AR060388 and CA052607 to DRR), a Young Investigator Career Development Award from the PKD foundation (02YI08A to AL), a Pilot and Feasibility Award from the SDRC of University of Colorado Denver (AR057212), and the REACH program of Stony Brook University (U01HL127522).

References

1. Park WJ, Liu J, Sharp EJ, Adler PN. The *Drosophila* tissue polarity gene *inturned* acts cell autonomously and encodes a novel protein. *Development*. 1996; 122:961–969. [PubMed: 8631273]
2. Park TJ, Haigo SL, Wallingford JB. Ciliogenesis defects in embryos lacking *inturned* or *fuzzy* function are associated with failure of planar cell polarity and Hedgehog signaling. *Nat Genet*. 2006; 38:303–311. [PubMed: 16493421]
3. Chang R, Petersen JR, Niswander LA, Liu A. A hypomorphic allele reveals an important role of *inturned* in mouse skeletal development. *Dev Dyn*. 2015; 244:736–747. [PubMed: 25774014]
4. Heydeck W, Liu A. PCP effector proteins *inturned* and *fuzzy* play nonredundant roles in the patterning but not convergent extension of mammalian neural tube. *Dev Dyn*. 2011; 240:1938–1948. [PubMed: 21761479]
5. Zeng H, Hoover AN, Liu A. PCP effector gene *Inturned* is an important regulator of cilia formation and embryonic development in mammals. *Dev Biol*. 2010; 339:418–428. [PubMed: 20067783]
6. Dai D, Li L, Huebner A, Zeng H, Guevara E, Claypool DJ, et al. Planar cell polarity effector gene *Intu* regulates cell fate-specific differentiation of keratinocytes through the primary cilia. *Cell Death Diff*. 2013; 20:130–138.
7. Toriyama M, Lee C, Taylor SP, Duran I, Cohn DH, Bruel AL, et al. The ciliopathy-associated CPLANE proteins direct basal body recruitment of intraflagellar transport machinery. *Nat Genet*. 2016; 48:648–656. [PubMed: 27158779]
8. Gailani MR, Stahle-Backdahl M, Leffell DJ, Glynn M, Zaphiropoulos PG, Pressman C, et al. The role of the human homologue of *Drosophila* *patched* in sporadic basal cell carcinomas. *Nat Genet*. 1996; 14:78–81. [PubMed: 8782823]
9. Hahn H, Wicking C, Zaphiropoulos PG, Gailani MR, Shanley S, Chidambaram A, et al. Mutations of the human homolog of *Drosophila* *patched* in the nevoid basal cell carcinoma syndrome. *Cell*. 1996; 85:841–851. [PubMed: 8681379]
10. Xie J, Murone M, Luoh SM, Ryan A, Gu Q, Zhang C, et al. Activating Smoothed mutations in sporadic basal-cell carcinoma. *Nature*. 1998; 391:90–92. [PubMed: 9422511]
11. Oro AE, Higgins KM, Hu Z, Bonifas JM, Epstein EH Jr, Scott MP. Basal cell carcinomas in mice overexpressing sonic hedgehog. *Science*. 1997; 276:817–821. [PubMed: 9115210]
12. Goetz SC, Anderson KV. The primary cilium: a signalling centre during vertebrate development. *Nat Rev Genet*. 2010; 11:331–344. [PubMed: 20395968]
13. Singla V, Reiter JF. The primary cilium as the cell's antenna: signaling at a sensory organelle. *Science*. 2006; 313:629–633. [PubMed: 16888132]
14. Oh EC, Katsanis N. Cilia in vertebrate development and disease. *Development*. 2012; 139:443–448. [PubMed: 22223675]
15. Eggenschwiler JT, Anderson KV. Cilia and developmental signaling. *Annu Rev Cell Dev Biol*. 2007; 23:345–373. [PubMed: 17506691]
16. Han YG, Kim HJ, Dlugosz AA, Ellison DW, Gilbertson RJ, Alvarez-Buylla A. Dual and opposing roles of primary cilia in medulloblastoma development. *Nat Med*. 2009; 15:1062–1065. [PubMed: 19701203]

17. Wong SY, Seol AD, So PL, Ermilov AN, Bichakjian CK, Epstein EH Jr, et al. Primary cilia can both mediate and suppress Hedgehog pathway-dependent tumorigenesis. *Nat Med.* 2009; 15:1055–1061. [PubMed: 19701205]
18. Youssef KK, Van Keymeulen A, Lapouge G, Beck B, Michaux C, Achouri Y, et al. Identification of the cell lineage at the origin of basal cell carcinoma. *Nat Cell Biol.* 2010; 12:299–305. [PubMed: 20154679]
19. Youssef KK, Lapouge G, Bouvree K, Rorive S, Brohee S, Appelstein O, et al. Adult interfollicular tumour-initiating cells are reprogrammed into an embryonic hair follicle progenitor-like fate during basal cell carcinoma initiation. *Nat Cell Biol.* 2012; 14:1282–1294. [PubMed: 23178882]
20. Zilber Y, Babayeva S, Seo JH, Liu JJ, Mootin S, Torban E. The PCP effector Fuzzy controls ciliary assembly and signaling by recruiting Rab8 and Dishevelled to the primary cilium. *Mol Biol Cell.* 2013; 24:555–565. [PubMed: 23303251]
21. Zhang Z, Wlodarczyk BJ, Niederreither K, Venugopalan S, Florez S, Finnell RH, et al. Fuz Regulates Craniofacial Development through Tissue Specific Responses to Signaling Factors. *PLoS One.* 2011; 6:e24608. [PubMed: 21935430]
22. Gray RS, Abitua PB, Wlodarczyk BJ, Szabo-Rogers HL, Blanchard O, Lee I, et al. The planar cell polarity effector Fuz is essential for targeted membrane trafficking, ciliogenesis and mouse embryonic development. *Nat Cell Biol.* 2009; 11:1225–1232. [PubMed: 19767740]
23. Dai D, Zhu H, Wlodarczyk B, Zhang L, Li L, Li AG, et al. Fuz controls the morphogenesis and differentiation of hair follicles through the formation of primary cilia. *J Invest Dermatol.* 2011; 131:302–310. [PubMed: 20962855]
24. Cui C, Chatterjee B, Lozito TP, Zhang Z, Francis RJ, Yagi H, et al. Wdpcp, a PCP protein required for ciliogenesis, regulates directional cell migration and cell polarity by direct modulation of the actin cytoskeleton. *PLoS Biol.* 2013; 11:e1001720. [PubMed: 24302887]
25. Heydeck W, Zeng H, Liu A. Planar cell polarity effector gene Fuzzy regulates cilia formation and Hedgehog signal transduction in mouse. *Dev Dyn.* 2009; 238:3035–3042. [PubMed: 19877275]
26. Aszterbaum M, Beech J, Epstein EH Jr. Ultraviolet radiation mutagenesis of hedgehog pathway genes in basal cell carcinomas. *J Investig Dermatol Symp Proc.* 1999; 4:41–45.
27. Villumsen BH, Danielsen JR, Povlsen L, Sylvestersen KB, Merdes A, Beli P, et al. A new cellular stress response that triggers centriolar satellite reorganization and ciliogenesis. *EMBO J.* 2013; 32:3029–3040. [PubMed: 24121310]
28. DeRouen MC, Zhen H, Tan SH, Williams S, Marinkovich MP, Oro AE. Laminin-511 and integrin beta-1 in hair follicle development and basal cell carcinoma formation. *BMC Dev Biol.* 2010; 10:112. [PubMed: 21067603]
29. Wang GY, Wang J, Mancianti ML, Epstein EH Jr. Basal cell carcinomas arise from hair follicle stem cells in *Ptch1*(+/-) mice. *Cancer Cell.* 2011; 19:114–124. [PubMed: 21215705]
30. Grachtchouk M, Pero J, Yang SH, Ermilov AN, Michael LE, Wang A, et al. Basal cell carcinomas in mice arise from hair follicle stem cells and multiple epithelial progenitor populations. *J Clin Invest.* 2011; 121:1768–1781. [PubMed: 21519145]
31. Peterson SC, Eberl M, Vagnozzi AN, Belkadi A, Veniaminova NA, Verhaegen ME, et al. Basal cell carcinoma preferentially arises from stem cells within hair follicle and mechanosensory niches. *Cell Stem Cell.* 2015; 16:400–412. [PubMed: 25842978]
32. Sanchez-Danes A, Hannezo E, Larsimont JC, Liagre M, Youssef KK, Simons BD, et al. Defining the clonal dynamics leading to mouse skin tumour initiation. *Nature.* 2016; 536:298–303. [PubMed: 27459053]
33. Von Hoff DD, LoRusso PM, Rudin CM, Reddy JC, Yauch RL, Tibes R, et al. Inhibition of the hedgehog pathway in advanced basal-cell carcinoma. *N Eng J Med.* 2009; 361:1164–1172.
34. Atwood SX, Sarin KY, Whitson RJ, Li JR, Kim G, Rezaee M, et al. Smoothed variants explain the majority of drug resistance in basal cell carcinoma. *Cancer Cell.* 2015; 27:342–353. [PubMed: 25759020]
35. Metcalfe C, de Sauvage FJ. Hedgehog fights back: mechanisms of acquired resistance against Smoothed antagonists. *Cancer Res.* 2011; 71:5057–5061. [PubMed: 21771911]

36. Priel S, Cortelazzi B, Dal Col V, Marson D, Laurini E, Fermeglia M, et al. Smoothened (SMO) receptor mutations dictate resistance to vismodegib in basal cell carcinoma. *Mol Oncol.* 2015; 9:389–397. [PubMed: 25306392]
37. Basset-Seguin N, Sharpe HJ, de Sauvage FJ. Efficacy of Hedgehog pathway inhibitors in Basal cell carcinoma. *Mol Cancer Ther.* 2015; 14:633–641. [PubMed: 25585509]
38. Atwood SX, Chang AL, Oro AE. Hedgehog pathway inhibition and the race against tumor evolution. *J Cell Biol.* 2012; 199:193–197. [PubMed: 23071148]
39. Wong SY, Dlugosz AA. Basal cell carcinoma, Hedgehog signaling, and targeted therapeutics: the long and winding road. *J Invest Dermatol.* 2014; 134:E18–22.
40. Kim J, Tang JY, Gong R, Kim J, Lee JJ, Clemons KV, et al. Itraconazole, a Commonly Used Antifungal that Inhibits Hedgehog Pathway Activity and Cancer Growth. *Cancer Cell.* 2010; 17:388–399. [PubMed: 20385363]
41. Infante P, Alfonsi R, Botta B, Mori M, Di Marcotullio L. Targeting GLI factors to inhibit the Hedgehog pathway. *Trends Pharmacol Sci.* 2015; 36:547–558. [PubMed: 26072120]
42. Kim DJ, Kim J, Spaunhurst K, Montoya J, Khodosh R, Chandra K, et al. Open-label, exploratory phase II trial of oral itraconazole for the treatment of basal cell carcinoma. *J Clin Oncol.* 2014; 32:745–751. [PubMed: 24493717]
43. Yasuda M, Claypool DJ, Guevara E, Roop DR, Chen J. Genetic manipulation of keratinocyte stem cells with lentiviral vectors. *Methods Mol Biol.* 2013; 989:143–151. [PubMed: 23483393]
44. Zeng H, Jia J, Liu A. Coordinated Translocation of Mammalian Gli Proteins and Suppressor of Fused to the Primary Cilium. *PLoS One.* 2011; 5:e15900.
45. Yuspa SH, Kilkenny AE, Steinert PM, Roop DR. Expression of murine epidermal differentiation markers is tightly regulated by restricted extracellular calcium concentrations in vitro. *J Cell Biol.* 1989; 109:1207–1217. [PubMed: 2475508]

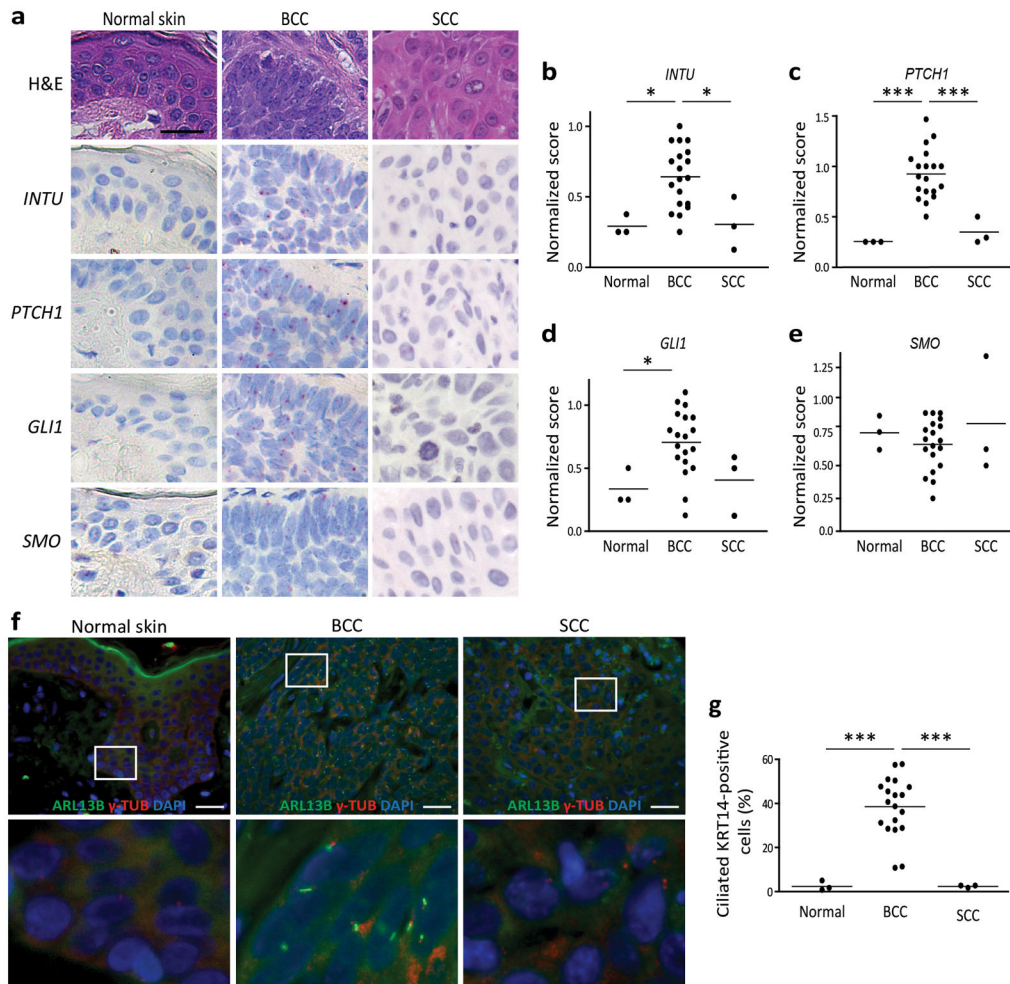


Figure 1.

INTU, Hh signaling, and primary cilia in healthy skin, BCC, and SCC. **(a)** Representative H&E staining and *in situ* hybridization of *INTU*, *PTCH1*, *GLI1*, and *SMO* in healthy adult human skin (normal skin), BCC, and SCC. **(b – e)** Normalized scores of signal intensity of *in situ* hybridization in **(a)**. **(f)** Representative images of primary cilia (ARL13B, green) and basal body (γ -tubulin (TUB), red) in normal skin, BCC, and SCC. Nuclei were stained with DAPI (blue). Lower panels are enlarged boxed areas above. **(g)** Percentage of ciliated keratinocytes in specimens in **(f)**. n = 3 for normal adult skin or SCC, n = 19 for BCC. *, $P < 0.05$; ***, $P < 0.001$, two-way ANOVA and pair-wise posttest. Scale bar = 25 μ m.

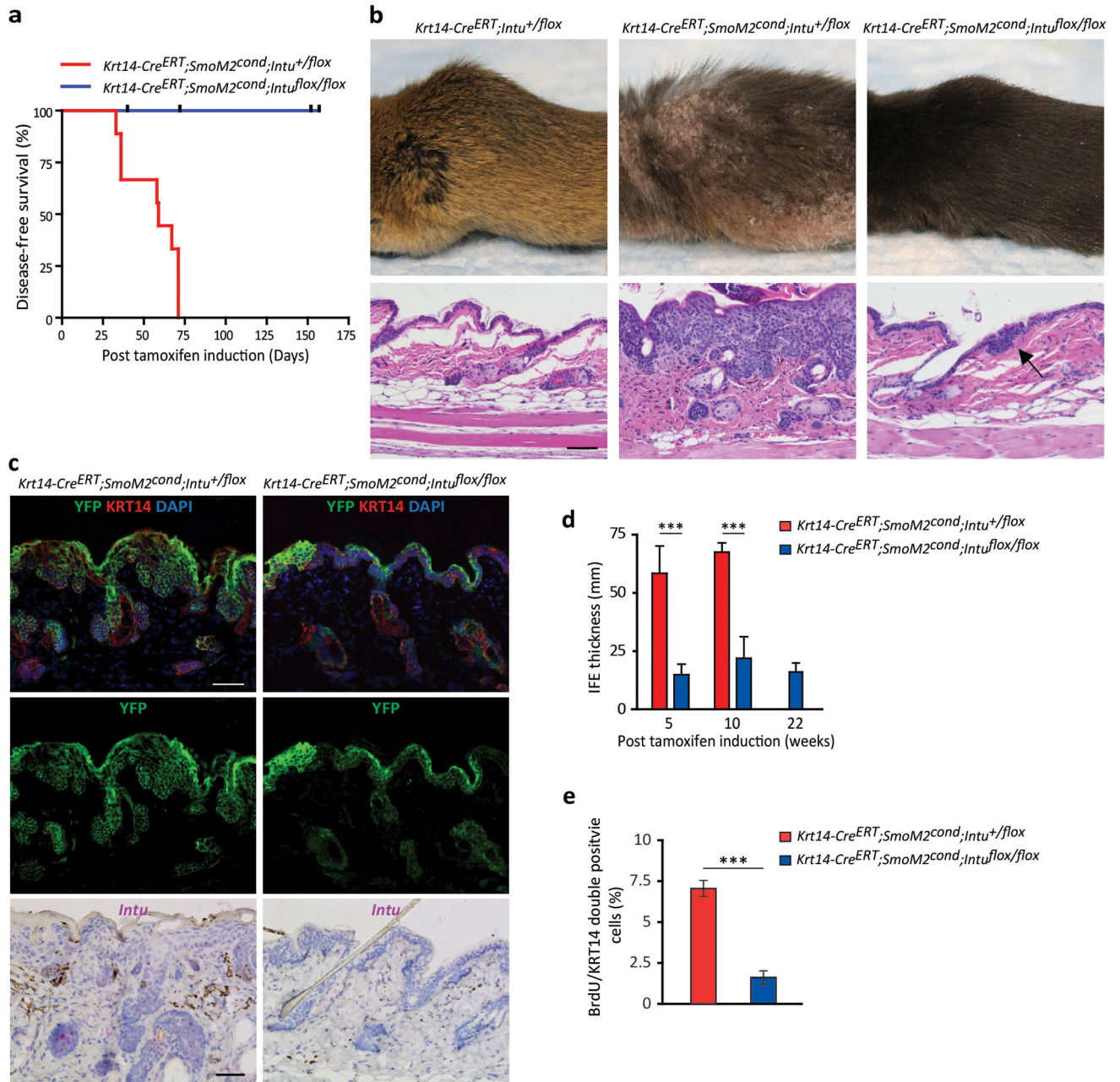


Figure 2. Disrupting *Intu* blocks BCC formation in mice. **(a)** Disease-free survival of *SmoM2*-driven BCC mouse models. Control, *Krt14-Cre^{ERT};SmoM2^{cond};Intu^{+/flox}* (n=9); homozygous *Intu* mutants, *Krt14-Cre^{ERT};SmoM2^{cond};Intu^{flox/flox}* (n = 14). ***, $P < 0.0001$, Logrank test. **(b)** Representative gross appearance (upper panels) and H&E staining (lower panels) of the dorsal skin harvested 10 weeks after tamoxifen induction. Arrow points to a focal epidermal invagination. **(c)** Immunofluorescence images of YFP (green) in dorsal skin of control and homozygous mouse models in (B). KRT14 was labeled red. Nuclei stained with DAPI (blue). **(d)** Thickness of interfollicular epidermis (IFE) of specimens in (B). Mean \pm SD.

***, $P < 0.001$, posttest, two-way ANOVA. (e) Percentage of BrdU and KRT14 double positive cells in specimens in (B). Mean \pm SD. ***, $P < 0.001$, T-Test. Scale bar = 50 μm .

Author Manuscript

Author Manuscript

Author Manuscript

Author Manuscript

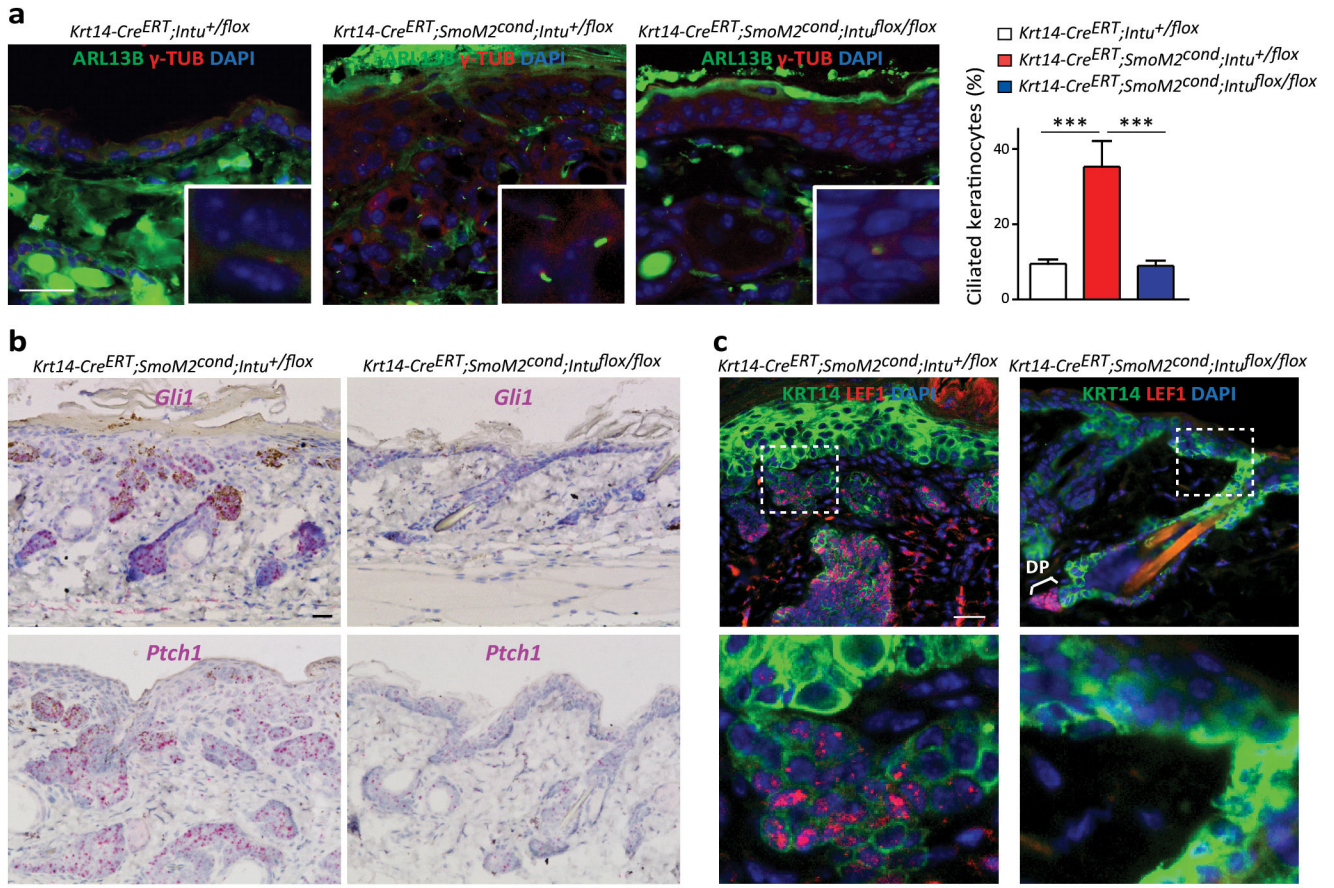


Figure 3.

Primary cilia, Hh and Wnt signaling in BCC mouse models. **(a)** Immunofluorescence labeling of primary cilia (ARL13B, green) and basal body (γ -tubulin (TUB), red) in dorsal skin of control (*Krt14-Cre^{ERT};SmoM2^{cond};Intu^{+/flox}*, n = 4, and homozygous (*Krt14-Cre^{ERT};SmoM2^{cond};Intu^{+/flox}*, n = 4) BCC mouse models and control mice (*Krt14-Cre^{ERT};Intu^{+/flox}*, n = 3), and quantification of ciliated keratinocytes. A minimum of 150 keratinocytes were evaluated per mouse. ***, $P < 0.001$, two-way ANOVA and pair-wise posttest. Nuclei were stained with DAPI (blue). **(b)** *In situ* hybridization of *Gli1* and *Ptch1* in dorsal skin obtained from specimens in **(a)**. **(c)** Immunofluorescence labeling of LEF1 (red) in dorsal skins obtained from specimens in **(a)**. Keratinocytes were labeled with KRT14 (green). Nuclei were staining with DAPI (blue). Lower panels are enlarged boxed areas above. Scale bar = 25 μ m.

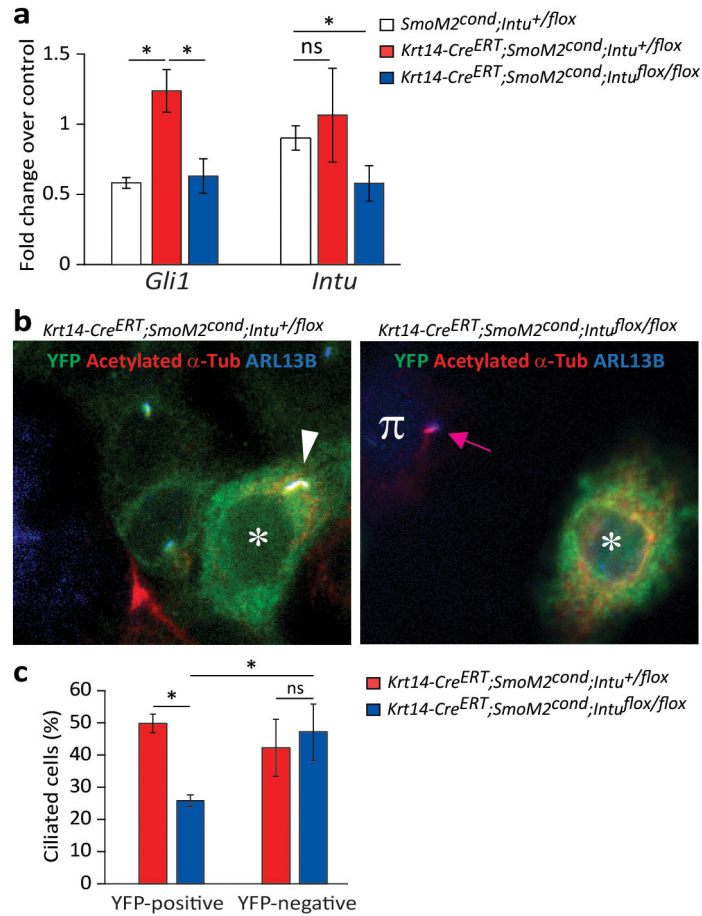


Figure 4.

Hh signaling and primary cilia in primary epidermal keratinocytes expressing *SmoM2*. (a) Relative transcription levels of *Gli1* and *Intu* in primary keratinocytes treated with 4-OH tamoxifen. n=3, *, $P < 0.05$, one-way ANOVA and posttest. (b) Representative immunofluorescence labeling of YFP (green) and primary cilia (acetylated α -tubulin (TUB), red, and ARL13B, blue) in 4-OH tamoxifen induced keratinocytes isolated from control (*Krt14-Cre^{ERT};SmoM2^{cond};Intu^{+/flox}*) and homozygous (*Krt14-Cre^{ERT};SmoM2^{cond};Intu^{flox/flox}*) mouse models. n = 3 per genotype. Arrowhead points to a triple positive cilium in an induced cell; arrow points to a cilium in an uninduced cell. (c) Statistical analysis of ciliated cells based on the expression of YFP as shown in (b).

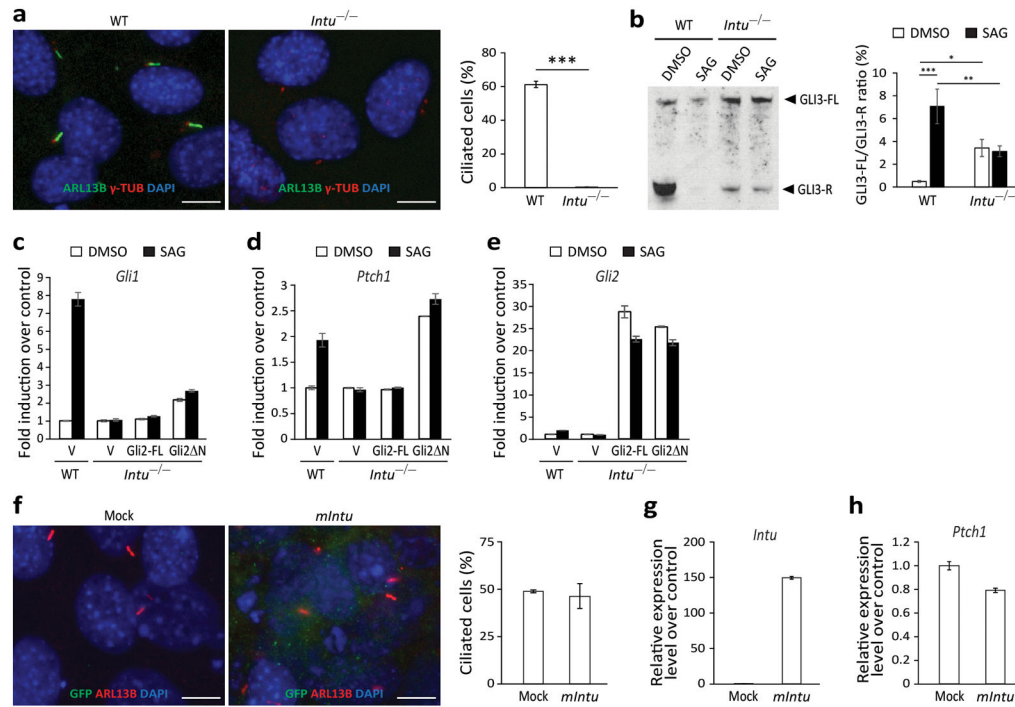


Figure 5. Effects of the expression levels of *Intu* on ciliogenesis and Hh signaling. **(a)** Primary cilia (ARL13B, green) and basal body (γ -tubulin, red) in wild type (WT) and *Intu*^{-/-} mouse embryonic fibroblasts (MEFs). **(b)** The relative expression levels of full-length GLI3 (GLI3-FL) and GLI3 repressor (GLI3-R) in DMSO and SAG-treated WT and *Intu*^{-/-} MEFs, and quantification (right). n = 3. *, *P* < 0.05; **, *P* < 0.01; ***, *P* < 0.001, two-way ANOVA and pair-wise post analysis. **(c – e)** Expression of *Gli1* **(c)**, *Ptch1* **(d)**, and *Gli2* **(e)** in WT and *Intu*^{-/-} MEFs in response to the overexpression of full-length *Gli2* (Gli2-FL) and a constitutively active *Gli2* (Gli2 Δ N), and SAG in a representative experiment. Vehicle (V) treated cells were used as controls. n = 4. **(f)** Primary cilia (ARL13B, green) in WT MEFs transfected with mouse *Intu*-GFP cDNA (*mIntu*), and quantification (right). **(g – h)** Relative expression levels of *Intu* and *Ptch1* in *mIntu*-transfected MEFs. Mock transfected cells were used as controls. n = 4. Scale bar = 10 μ m.